

of ω_0 are present, one finds "coherences," or "echoes" as described in the following paper.

VIII. GENERALIZATION FOR $T_1 \neq T_2$

The assumption that the two relaxation times are equal has simplified our geometric interpretations, but the analytical expressions in the 3×3 representation remain almost as simple if it is dropped. Thus, the equation of motion (3) remains valid provided we

interpret $1/T$ as a diagonal matrix with elements $[1/T_2, 1/T_2, 1/T_1]$. Equations (4), (5), (16) then remain valid although $\mathbf{R}(t, t')$ is no longer a pure rotation matrix. The time-development matrix $\mathbf{U}(t, t')$ is given by an expression of the form (8) in which β is replaced by $(\mathbf{T}^{-1} + \beta)$, and the solution (13) is valid, with $\lambda(t) = \exp[-(\mathbf{T}^{-1} + \beta)t]$. The locus generated by $\lambda(t)$ is now a distorted version of a cone. Similarly, the relations (22)–(26) of Sec. IV still hold, although the geometrical picture is less simple.

Nuclear Induction in Inhomogeneous Fields*

ARNOLD L. BLOOM
Varian Associates, Palo Alto, California
 (Received December 20, 1954)

The mathematical methods developed by Jaynes are applied to the study of nuclear resonance in inhomogeneous magnetic fields. It is shown that a description of delayed-signal phenomena such as spin echoes is greatly simplified by the use of the spinor representation involving 2×2 transformation matrices. The original results of Hahn on spin echoes are rederived in simplified fashion and more complicated situations are discussed, including large numbers of pulses, exact time dependence in extremely inhomogeneous fields, and continuous pulse trains. Several previously unreported types of delayed-signal phenomena are discussed and illustrated experimentally by oscilloscope traces. The apparatus used to study nuclear induction in very inhomogeneous fields is briefly discussed.

I. INTRODUCTION

THIS report applies the mathematical methods developed in the previous paper¹ to the study of nuclear induction in inhomogeneous magnetic fields, involving a class of phenomena such as spin echoes.² In previous papers on spin echoes²⁻⁵ the analysis always involved successive operations in the three-dimensional rotation group, and the use of linear transformation operators was implied even if these operators were not always written in matrix format. It is thus not our intention merely to demonstrate the use of matrices for predicting spin echoes. What we wish to accomplish is the following: (1) to demonstrate the use of Cayley-Klein parameters in spin-echo problems, and (2) to show how the simplicity and generality of the Cayley-Klein formalism makes it possible to study more complicated situations with a minimum of effort.

II. MATHEMATICAL PRELIMINARIES

We shall assume that the reader is familiar with the original spin-echo experiments of Hahn,² and with the

mathematical and geometrical interpretations presented in the Hahn paper. We shall follow the same general method of attack. Starting with a vector $\mathbf{M}(\Delta\omega)$ which obeys Bloch's⁶ equations [Eqs. (1) or (3) of I] and which is initially in the z direction, we perform successive transformations corresponding to discrete time intervals during which a given rf field H_1 is either present or absent. Finally, after all rf signals have been applied, the polarization in the xy plane takes the form,

$$M_{x-iy}(\Delta\omega) = g(\Delta\omega) \sum_j G_j(\Delta\omega) \exp[-i\Delta\omega(t-t_j)], \quad (1)$$

where g describes the effect of the magnetic field inhomogeneity and the G 's are functions of relaxation, self-diffusion and three-dimensional rotation; it is only the latter variable that is of interest to us. The observed nuclear induction signal depends on the integral of (1) over all values of $\Delta\omega$. In general the integral is zero unless t is in the vicinity of t_j , in which case there is a signal of intensity proportional to G_j . If t_j coincides with an rf pulse the signal is a "free decay," otherwise it is an "echo."

The transformation relations which are of interest to us have been given in Sec. VI of I. During the i th pulse the matrix Q_i is described as

$$Q_i = \begin{pmatrix} \alpha_i & \beta_i \\ -\beta_i^* & \alpha_i^* \end{pmatrix}, \quad (2)$$

* Supported by the Office of Naval Research.

¹ E. T. Jaynes, preceding paper [Phys. Rev. **98**, 1099 (1955)], hereafter referred to as I.

² E. L. Hahn, Phys. Rev. **80**, 580 (1950).

³ E. L. Hahn and D. E. Maxwell, Phys. Rev. **88**, 1070 (1952); D. E. Maxwell, thesis, Stanford University (unpublished).

⁴ T. P. Das and A. K. Saha, Phys. Rev. **93**, 749 (1954).

⁵ H. Y. Carr and E. M. Purcell, Phys. Rev. **94**, 630 (1954).

⁶ F. Bloch, Phys. Rev. **70**, 460 (1946).

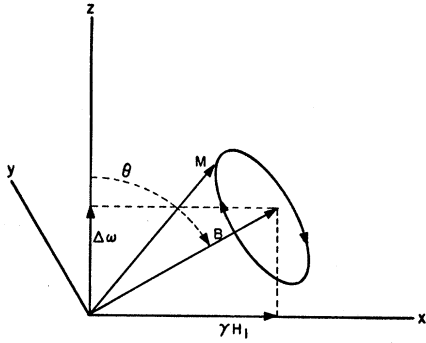


FIG. 1. Diagram of the vectors \mathbf{M} , \mathbf{B} and the precession cone in the rotating frame of reference.

in which⁷ (omitting subscripts for the moment),

$$\begin{aligned}\alpha &= \cos(\frac{1}{2}bt) - i \cos\theta \sin(\frac{1}{2}bt), \\ \beta &= -i \sin\theta \sin(\frac{1}{2}bt),\end{aligned}\quad (3)$$

where the asterisk denotes the complex conjugate, and

$$\begin{aligned}b &= |\mathbf{B}|, \\ \mathbf{B} &= \gamma\mathbf{H}_1 + \Delta\omega, \\ \theta &= \tan^{-1}(\gamma H_1 / \Delta\omega), \\ \Delta\omega &= \gamma\mathbf{H}_0 - \omega.\end{aligned}\quad (4)$$

The precession is clockwise for $\gamma > 0$ when viewed from in front of the effective field vector \mathbf{B} (see Fig. 1). In between pulses we have the special case

$$Q = \begin{pmatrix} e^{-\frac{1}{2}i\Delta\omega t} & 0 \\ 0 & e^{\frac{1}{2}i\Delta\omega t} \end{pmatrix}, \quad (5)$$

corresponding to precession about the z axis with angular frequency $\Delta\omega$. The resultant transformation after n time intervals is then defined as

$$Q = Q_n \cdots Q_1 = \begin{pmatrix} \alpha & \beta \\ -\beta^* & \alpha^* \end{pmatrix}. \quad (6)$$

To convert Q to a three-dimensional representation, we use Eq. (40) of **I**, which we summarize as follows:

$$\begin{pmatrix} M'_{x+iy} \\ M'_{x-iy} \\ M'_z \end{pmatrix} = \begin{pmatrix} \alpha^{*2} & -\beta^{*2} & -2\alpha^*\beta^* \\ -\beta^2 & \alpha^2 & -2\alpha\beta \\ \alpha^*\beta & \alpha\beta^* & (\alpha\alpha^* - \beta\beta^*) \end{pmatrix} \begin{pmatrix} M_{x+iy} \\ M_{x-iy} \\ M_z \end{pmatrix}. \quad (7)$$

Thus, starting with $M = M_z$ we wish to compute M_{x-iy} at a later time, i.e., the matrix element $(-2\alpha\beta)$ as a function of t . From inspection of Eqs. (2), (5), and (6), we see that $(-2\alpha\beta)$ can be written in the form

$$-2\alpha\beta = \sum_j G_j \exp[-i\Delta\omega(t-t_j)], \quad (8)$$

which is in the form needed to study spin echoes.

⁷ All computations in this paper are carried out in the rotating frame of reference, in which H_1 is taken to be always in the x direction. See Rabi, Ramsey, and Schwinger, *Revs. Modern Phys.* **26**, 167 (1954).

To summarize, we compute α and β by combining the 2×2 Q -matrices and multiply these two parameters together to obtain the required three-dimensional matrix element. This procedure is generally much simpler than that of multiplying 3×3 matrices directly, and many of the results which were laboriously computed in the earlier papers can be determined merely by a visual inspection of the Q -matrices. In addition the generality of the Cayley-Klein parameters allows us to waive the restrictions (nuclei at resonance, short and intense pulses of rf) which were necessary in the earlier work in order to keep the computations to a manageable length.

III. GENERAL ANALYSIS

A. Introduction

In this section, we shall calculate the amplitudes and shapes of signals in an idealized situation in which both T_1 and T_2 (if they are not equal) are very long compared to the times required to do the experiments, and in which self-diffusion effects are absent. For each instant of time we must solve the corresponding Eq. (13) of **I**, which can be written in the form

$$\mathbf{M}(t) = [e^{-t/T} \exp(-\beta t)] \mathbf{M}_1 + [1 - e^{-t/T} \exp(-\beta t)] \mathbf{M}_2. \quad (9)$$

Here $T_1 = T_2 = T$, \mathbf{M}_1 is the polarization at the start of the time interval, \mathbf{M}_2 is the steady-state polarization for that interval, and β is the precession matrix.⁸ It is customary in treatments of spin echo²⁻⁵ to assume an initial polarization $\mathbf{M} = M_0 \mathbf{z}$ prior to the first pulse, and to solve only for the first term in (9), ignoring the effect of \mathbf{M}_2 . The neglect of this second term during the time between pulses, when it corresponds to a recovery of initial polarization, is justifiable only for long relaxation times; actually the recovery is quite useful for the measurement of T_1 . Neglect of $[1 - e^{-t/T} \exp(-\beta t)] \mathbf{M}_2$ during a pulse is not so easily justified. In most spin-echo experiments, however, the rf level, if left on continuously, would correspond to a high degree of saturation; in such cases it can be shown that \mathbf{M}_2 is either very small or is nearly parallel to \mathbf{B} , so the total effect of the term is small. We shall follow the usual practice of neglecting the term in \mathbf{M}_2 ; it is nevertheless clear that there are circumstances under which one cannot neglect \mathbf{M}_2 , even for relatively short pulses and intense rf fields.

We shall make no assumptions in this section about the magnetic field inhomogeneity effect, $g(\Delta\omega)$, except to follow the usual practice in requiring $g(\Delta\omega) = g(-\Delta\omega)$. An inspection of the basic equations of motion and of Fig. 1 shows that if the initial polarization is in the z direction the two vectors for each $|\Delta\omega|$ are at all times symmetrically located about the yz plane, from which it follows that $G_j(\Delta\omega) = -G_j^*(-\Delta\omega)$. Thus if the above restriction on g is fulfilled it is only necessary to use the

⁸ In this paper α and β refer to transformation operators as defined in Eqs. (2) and (22) of **I**. The corresponding lightface characters are the Cayley-Klein parameters.

imaginary part of G_j in computing signal amplitudes and shapes.

When the transformation matrices are displayed it is fairly evident how one may modify them to include the effects of relaxation and self-diffusion. These effects have already been calculated in detail for two- and three-pulse systems⁴ and it does not appear that their applications to more complex systems will produce much that is physically new or interesting. Exceptions to this latter statement will be discussed qualitatively.

B. One, Two, and Three Pulses

In order to show in a simple manner how our method of calculation works, we shall first rederive Hahn's results² for maximum amplitudes of signals following one, two, and three pulses in the absence of relaxation and self-diffusion effects. The notation refers to the time intervals as defined in Fig. 2. Odd numbered subscripts refer to pulses, even numbered subscripts to intervals between pulses. All times are measured from the beginning of the time interval, rather than from the start of the experiment.

1. *One pulse.*—The term $(-2\alpha\beta)$ in the matrix $Q=Q_2Q_1$ is given by

$$(-2\alpha\beta) = -2\alpha_1\beta_1 e^{-i\Delta\omega t_2}, \quad (10)$$

and substituting Eq. (3) we have

$$(-2\alpha\beta) = [\sin 2\theta \sin^2(\frac{1}{2}bt_1) + i \sin\theta \sin bt_1] e^{-i\Delta\omega t_2}. \quad (11)$$

The only signal during this time interval is the free decay following the pulse ($t_2=0$). Near resonance the term $\sin\theta \sin bt_1$ is adequate to describe the free decay amplitude as a function of pulse parameters.

2. *Two pulses.*—The term $(-2\alpha\beta)$ in the matrix $Q=Q_4\cdots Q_1$ is given by

$$(-2\alpha\beta) = -2(\alpha_1\alpha_3 e^{-2-4} - \beta_1^*\beta_3 e^{+2-4}) \times (\beta_1\alpha_3 e^{-2-4} - \alpha_1^*\beta_3 e^{+2-4}), \quad (12)$$

where e^{-2} is short for $\exp(-\frac{1}{2}i\Delta\omega t_2)$, e^{+4} for $\exp(+\frac{1}{2}i\Delta\omega t_4)$, etc. Of the four terms in (12) one of them refers to times which are negative with respect to the second pulse and which we shall disregard. The other two represent coherences at $t_4=0$ (free decay of the second pulse), and at $t_4=t_2$, which is the simple two-pulse echo. Substituting (3) into the coefficient for the free decay, we obtain for the free decay amplitude

$$G_1 = -(\alpha_1\alpha_1^* - \beta_1\beta_1^*)(2\alpha_3\beta_3). \quad (13)$$

The amplitude of the echo is given by

$$G_2 = 2\alpha_1^*\beta_1^*\beta_3^2. \quad (14)$$

For pulses of equal intensity and width, and nuclei near resonance, (14) reduces to

$$G_2 = \sin bt_1 \sin^2(\frac{1}{2}bt_1), \quad (15)$$

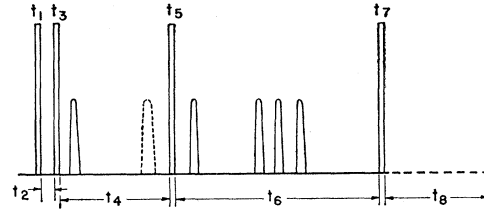


FIG. 2. Timing diagram for up to four unequally spaced pulses.

in agreement with the result calculated by Hahn. Note, however, that Eq. (14) is quite general and with very little extra labor will give the echo amplitude for pulses of different width and intensity, and for nuclei not near resonance. [See for example Eq. (28).]

3. *Three pulses with $t_4 > t_2$.*—In the matrix $Q=Q_6\cdots Q_1$ both α and β consist of four terms with the following exponents:

$$e^{-2-4-6}, e^{-2+4-6}, e^{+2-4-6}, e^{+2+4-6}.$$

When we multiply these together to obtain $(-2\alpha\beta)$, we obtain ten terms (signals) corresponding to the combinations of the above terms taken two at a time. Of these ten terms, two occur at $t_6=0$ and represent the free decay following the third pulse. Of the remaining eight terms, four must occur at negative time t_6 , which we temporarily disregard, and four at positive time, which predict echos. The times of the echos, and the terms which give their intensity, are as follows:

At $t_6=t_2$ (stimulated echo)

$$G_2 = 4\alpha_1^*\beta_1^*\alpha_3^*\beta_3\alpha_5\beta_5, \quad (16)$$

at $t_6=t_4-t_2$

$$G_3 = -2\alpha_1\beta_1\beta_3^*\beta_5^2, \quad (17)$$

at $t_6=t_4$

$$G_4 = 2(\alpha_1\alpha_1^* - \beta_1\beta_1^*)\alpha_3^*\beta_3^*\beta_5^2, \quad (18)$$

at $t_6=t_4+t_2$

$$G_5 = 2\alpha_1^*\beta_1^*\alpha_3^*\beta_5^2. \quad (19)$$

By substitution of the definitions, Eqs. (3), one finds that these expressions reduce to the ones given by Hahn for the special case which he considers.

C. Three Equally Spaced Pulses

The numbers of echos and their amplitudes are also a function of the positions of the pulses. Previously we were careful to state that the third pulse should occur after the simple echo following the first two pulses. Obviously, if the third pulse occurs too soon, certain "echos of echos" cannot occur and the amplitudes and the numbers of the echos following the third pulse will be different. This has been briefly mentioned by Hahn.² Here we will discuss a special case, that of three equally spaced pulses ($t_2=t_4$). In this particular case there will be only two echos following the third pulse and these echos will be spaced so as to continue the original pulse train.

The details of the calculations are the same as in the preceding cases and we shall merely state the result for

the coefficient of the echo which occurs at a time t_2 (or t_4) following the third pulse, i.e., the first of the two echoes. This coefficient is given by

$$G = 2[2\alpha_1^* \beta_1^* \alpha_3^* \beta_3 \alpha_5 \beta_5 + (\alpha_1 \alpha_1^* - \beta_1 \beta_1^*) \alpha_3^* \beta_3^* \beta_5^2]. \quad (20)$$

The first term we recognize from (16) to be the coefficient for the three-pulse "stimulated" echo. In the second term, the first section $(\alpha_1 \alpha_1^* - \beta_1 \beta_1^*)$ we recognize from (7) to be the matrix element which leaves the z component unchanged; the rest of this term is the formula for the two-pulse echo produced by the second and third pulses. Thus the echo is merely the direct sum of two superimposed echoes. One might think that such a direct sum of echoes would be likely under certain conditions to give an amplitude greater than the original polarization; however, an analysis of the coefficients shows that this is not so.

D. More Than Three Pulses

In his original article, Hahn² pointed out the existence of two-pulse and three-pulse (stimulated) echoes. It was of interest in connection with this project to find out if these were the only types of echoes that could be produced, or if there were also echoes that could be understood in terms of four or more pulses. We shall not try to prove the existence of n -pulse echoes for any n but shall investigate the possibility that there exist four-pulse echoes, which will imply that there may exist echoes that could be formed only with $n > 4$ pulses.

We suppose that the four pulses are spaced so that all echoes which can be produced by any one set of pulses occur before the next pulse is applied (Fig. 2). In the final transformation the matrix elements α, β each consist of eight terms which, taken two at a time and combining similar exponents, gives a total of 36 terms in the product $-2\alpha\beta$. Of these terms, four occur at $t_8 = 0$ and represent the free decay following the fourth pulse. The remaining terms are located symmetrically about $t_8 = 0$ giving 16 terms prior to the fourth pulse, which we disregard, and 16 positive corresponding to echoes. Before going any further, let us return for a moment to the case of three unequally spaced pulses. We noted that there must be four coherence terms for $t_6 < 0$, symmetric about the third pulse with respect to the four echoes in t_6 . However, there are only three actual coherences in the time prior to the third pulse. The extra term, shown

by a dotted line in Fig. 2, is therefore a "virtual" echo that does not exist until the third pulse is applied, but following the third pulse the nuclear system behaves in every way as if the virtual echo had actually occurred.

If we include the virtual echo among the sources of two- and three-pulse echoes following the fourth pulse, we get a total of 14 such echoes. This still leaves two echoes unaccounted for, which must be four-pulse or "super-stimulated" echoes.

The analysis can be extended readily to n pulses. If all pulse spacings are unequal, and if

$$t_{2n-2} > t_2 + t_4 + \dots + t_{2n-4},$$

as before, then, following the n th pulse there will be 2^{2n-4} echoes. Since the total number of coherences, real and virtual, due to the $(n-1)$ st pulse is $2(2^{2n-6}) + 1$, the n th pulse must create $(2^{2n-5} - 1)$ new virtual coherences.

E. Sets of Double Pulses

A special case of four pulses which is of particular interest is that of a two-pulse spin-echo experiment repeated in a time of the order of T_1 or less, so that the sample still has some memory of the previous set of two pulses. In this case one usually observes at least one additional echo, marked S in Fig. 3, following the primary echo. The origin of this echo is as follows: The third pulse (Fig. 3) creates a virtual echo, V , which is mathematically similar to the stimulated echo which would occur at the position occupied by the fourth pulse. The latter pulse, however, transforms V into a two-pulse echo at S . That this analysis is essentially correct can be seen by calculating the coefficient for this echo. The calculation gives

$$G_S = -4\alpha_1^* \beta_1^* \alpha_3^* \beta_3 \alpha_5^* \beta_5^* \beta_7^2, \quad (21)$$

which is a stimulated echo transformed by another pulse.

As can be seen from its genesis, this secondary echo has many properties in common with Hahn's stimulated echo. In particular, its amplitude is more nearly dependent on T_1 than on T_2 and is relatively immune to self-diffusion effects. Experimentally, if the signal-to-noise ratio is high, this echo can often be seen even when the time between double pulses is several times T_1 .

In the vicinity of resonance, and for pulses of equal length and intensity, Eq. (21) reduces to

$$G_S = \frac{1}{2} \sin^3(bt_1) \sin^2(\frac{1}{2}bt_1), \quad (22)$$

which has its maximum at $\cos bt_1 = -\frac{1}{4}$. If the experimental repetition rate is fast enough, additional echoes can be seen following S which can be explained in terms of virtual echoes of S on pulse three, etc. In some cases real echoes can be seen preceding the pulses as well as following them, but these must be explained by the symmetry property discussed in the section on continuous pulse trains.

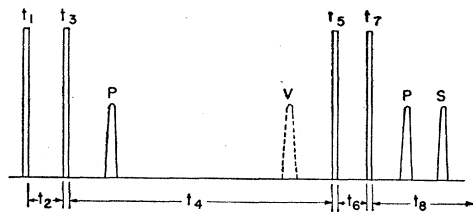


FIG. 3. Diagram for problem of repeated double pulses.

IV. VERY INHOMOGENEOUS FIELDS

A. Introduction

In the original spin-echo experiments² performed in fields that were only slightly inhomogeneous, it was shown that: (1) The spacing between second pulse and echo was approximately the same as between first and second pulse. (2) The free decay was the Fourier transform of the moment distribution $g(\Delta\omega)$ in the magnetic field. (3) The echo was shaped like two free decays placed back-to-back.

In this section we shall consider a somewhat different case, that of a magnetic field so inhomogeneous that the total inhomogeneity, $\gamma\Delta H$, is very much greater than the frequency spectrum of the pulses. We shall assume an "infinite flat-topped" distribution [$g(\Delta\omega)$ constant for all $\Delta\omega$], thus the exact locations and shapes of signals will depend on the Fourier transforms of the $G_j(\Delta\omega)$. As explained previously, it is only necessary to compute the imaginary parts of the G 's.

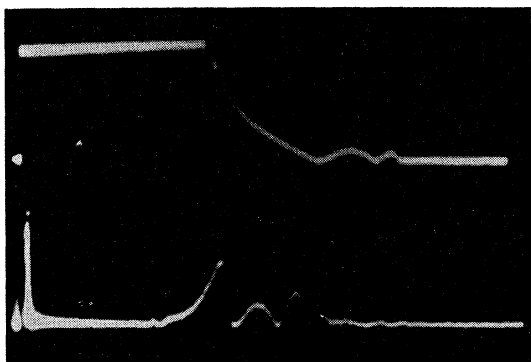


FIG. 4. Free decay (above) and echo (below) when $\gamma H_1 t_1 \approx 4\pi$.

B. Free Decay

The shape of the free decay can be deduced from the imaginary part of Eq. (11):

$$\text{Im}[G(\Delta\omega)] = \sin\theta \sin bt_1 \cos\Delta\omega t_2 - \sin 2\theta \sin^2(\frac{1}{2}bt_1) \sin\Delta\omega t_2, \quad (23)$$

where $\theta = \theta(\Delta\omega)$ is given by Eq. (4). The frequency spectrum of the free decay is determined in this case not by the field inhomogeneity but by the rf level. Thus for a given value of $\gamma H_1 t_1$ a long pulse of weak rf amplitude will have a long free decay and a short pulse of strong rf will have a short decay.

It is possible to write (23) in the form

$$\text{Im}G = \cos\Delta\omega t \cos\Delta\omega t_2 + \sin\Delta\omega t \sin\Delta\omega t_2, \quad (24)$$

where the maximum signal presumably occurs at $t_2 = t$. A little algebra gives

$$\tan\Delta\omega t = -\cos\theta \tan(\frac{1}{2}bt_1). \quad (25)$$

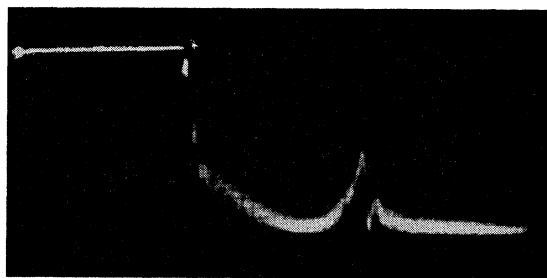


FIG. 5. Free decay and edge echo following single pulse. The pulses were repeated in a time short compared to T_2 .

From (25) we see that there is no one instant of time when all components are exactly in phase. However, we can determine a time (prior to the end of the pulse) when the free decay, projected back to this time, would have had its maximum value. If $\gamma H_1 t_1 \leq 1$ and we consider only the components about resonance, we can approximate (25) by

$$\Delta\omega t = -\frac{1}{2}bt_1 \cos\theta, \quad (26)$$

and since $\cos\theta = \Delta\omega/b$ we have simply

$$t = -\frac{1}{2}t_1. \quad (27)$$

Thus the free decay behaves as if it had started from the midpoint of the pulse. When $\gamma H_1 t_1 \gg 1$, t is different for different groups of values of $\Delta\omega$, with the result that the free decay may show considerable structure. An example of such a free decay is shown in Fig. 4.

C. Edge Echo

The "edge echo" is a phenomenon observable only in a very inhomogeneous magnetic field. If a single square pulse of length t_1 is impressed on the nuclear moment ensemble in such a field, the edge echo appears as a small signal at a time t_1 after the end of the pulse. The effect becomes particularly noticeable for pulses repeated in a time short compared to T_2 and is illustrated in Fig. 5. The structure at the end of the free decay in Fig. 4 can also be considered in part as an edge echo.

The origin of the edge echo can be seen by inspection of Eq. (11). For nuclei far from resonance b is approximately equal to $\Delta\omega$, thus to this approximation (11) contains terms of the form $\exp[-i\Delta\omega(t_2 - t_1)]$. A coherence is thus produced by nuclei far from resonance at a time t_1 after the pulse termination. The shape of the edge echo can be inferred by substituting $\Delta\omega$ for b in (23); it has the form $\int \sin[\Delta\omega(t_2 - t_1)] d(\Delta\omega)$. The shape of this signal is not the single lobe usually associated with an echo. Instead, if detected by a phase-sensitive detector, it reaches a maximum, goes sharply through zero at $t_2 = t_1$, and goes through a maximum in the opposite direction. If the edge echo is viewed only in absolute value, it appears as two maxima separated by a sharp minimum, as shown in Fig. 5.

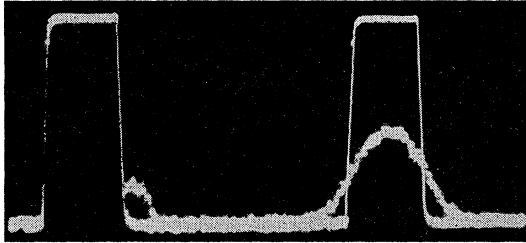


FIG. 6. Superpositions of first pulse, second pulse, and echo showing exact timing of echo maximum.

D. Two-Pulse Echo

For two pulses of equal H_1 the echo signal is obtained by substituting (4) into (14) and taking the imaginary part:

$$\begin{aligned} \text{Im}G_2 = & -\sin^2\theta \sin(bt_1) \sin^2(\frac{1}{2}bt_3) \cos[\Delta\omega(t_4-t_2)] \\ & -\sin 2\theta \sin^2\theta \sin^2(\frac{1}{2}bt_1) \\ & \times \sin^2(\frac{1}{2}bt_3) \sin[\Delta\omega(t_4-t_2)]. \end{aligned} \quad (28)$$

This differs considerably from (23) and the echo is therefore not the same as two free decays placed back-to-back. The common factor $\sin^2\theta$ in (28) cuts down the high-frequency terms in the echo, with the result that the echo is a considerably rounded-off version of the original square pulse. If we write (28) in the form $\cos[\Delta\omega(t_4-t_2-t)]$ we again get (26) and (27) as expressions for t . In other words, if we sweep the oscilloscope with repetition rate $(t_1+t_2)^{-1}$, where t_2 is the time between pulses, and if $\gamma H_1 t_1 = \gamma H_1 t_3 \leq 1$, we will find the echo maximum exactly at the center of the pulse. (See Fig. 6.) For $\gamma H_1 t_1 \gg 1$, the echo shape can get quite complicated (Fig. 4).

V. CONTINUOUS PULSE TRAINS

A. Introduction

In this section, we shall discuss the spin-echo type of solution for continuous trains of pulses. We can assume that the pulse trains start at some initial time $t=0$ and then continue for a time very much longer than the relaxation time T of the substance so that the sample has essentially forgotten when the beginning of the pulse train occurred. We shall follow the same assumptions as in the previous sections with regard to equality of relaxation times and negligible self-diffusion, except that when working with terms that represent infinite series it is necessary to include relaxation time explicitly in the formula in order to insure that the series converge. In what follows, we shall call the repetition time between successive cycles of pulses τ and other definitions shall be as in preceding discussions. We shall, in general, assume that pulse widths are short compared to τ and that $\tau \ll T$.

B. Symmetry with Respect to Time Inversions

One of the more interesting properties of the nuclear system when subjected to continuous pulse trains is the property of time symmetry. Consider the basic equations of motion for the polarization, such as Eq. (1) of I. If we make T large so that the relaxation term is small compared with the other terms in the equation, then reversal of the sign of t is equivalent to a reversal of the sign of the gyromagnetic ratio γ . Thus, if we go backward in time, any solutions which we obtain must also be solutions of Bloch's equations, except for the sign of γ which will make no difference in a system which does not detect phase.⁹ If we have an rf driving function which is an even function of time, then after the nuclear system has settled down to steady state it will make no difference whether we take time in the backward or forward direction. Thus the nuclear system must not only produce free decays and edge echoes following the pulses but must anticipate the pulses in exactly the same way. If the driving function consists of double pulses there will be echoes preceding and following the pulses. This property of anticipating the driving function is shown in Fig. 7. Actually, the signal shown in this figure is not perfectly symmetrical owing to self-diffusion effects.

C. End of a Train of Single Pulses

The solution of Bloch's equations for a continuous train of pulses has been given in I. If subscript 1 applies to the pulse, 2 to the interval between pulses, and t is the time following the last pulse, then the solution can be written as

$$\mathbf{M} = \mathbf{M}' \exp(-\beta_2 t), \quad (29)$$

$$\mathbf{M}' = \mathbf{M}_2(\infty) + (1-\alpha)^{-1}(1-\alpha_2)[\mathbf{M}_1(\infty) - \mathbf{M}_2(\infty)], \quad (30)$$

where (30) is just Eq. (35) of I with subscripts interchanged. It is, unfortunately, not possible to add three-dimensional rotation operators by performing any simple operation on the corresponding Q -matrices. Calculation of the solution must therefore be carried out with 3×3 matrices and becomes quite tedious. The solution can be written in the form⁸

$$M_{x-iy} = [\det(1-\alpha)]^{-1} (f + g e^{i\Delta\omega t_2} + h e^{-i\Delta\omega t_2}) e^{-i\Delta\omega t}, \quad (31)$$

where f , g , h are polynomials in α_1 , β_1 , and $e^{-\tau/T}$. Of interest to us is the effect of the denominator, which can be expanded in a power series as follows:

$$\begin{aligned} [\det(1-\alpha)]^{-1} & \propto \sum_{n=0}^{\infty} \\ & \times \left[\frac{(e^{-\tau/T} - e^{-2\tau/T})(\alpha_1^2 e^{-i\Delta\omega t_2} + \text{cc})}{(1-R_{33}e^{-\tau/T})(1-R_{33}e^{-2\tau/T})} \right]^n, \end{aligned} \quad (32)$$

⁹ This argument is similar to the symmetry property discussed by B. Jacobsohn and R. K. Wangness, Phys. Rev. **73**, 942 (1948). The argument shown there, valid for a weak, frequency-modulated rf signal, requires no assumptions about the magnitude of T_1 .

where $R_{33} = \alpha_1 \alpha_1^* - \beta_1 \beta_1^*$. From (31), (32), and Section IV-D (showing that the center of an echo is related to τ rather than to t_2) we see that the response of the nuclear system is a series of echoes spaced apart a time τ , in essence trying to extend the train of pulses. From (32) we see that the echoes decay exponentially with a decay constant which is a function of $\gamma H_1 t_1$, but not of elapsed time and only indirectly of relaxation time. In other words, the decay takes place in a certain number of pulse repetitions, rather than in a given elapsed time. This is illustrated in Fig. 8, which shows a decay which was independent of time even though τ was varied by a factor of three.

VI. EXPERIMENTAL APPARATUS

Although the spin-echo apparatus used in making the traces shown in Figs. 4-8 and in testing the theory generally was of fairly conventional design, a few words will be said concerning the characteristics and performance of this particular instrument. The apparatus employed a coherent source of 30 megacycles, consisting of a free-running crystal oscillator whose output was keyed after it had passed through several doubler and buffer stages. The rf pulses had a rise time of 10 microseconds and produced a maximum field, $2H_1$ at the sample, of about 10 gauss. Both rf intensity and pulse length were variable. The probe used crossed coils.¹⁰ The proton sample, about 25 cm³ in volume, was placed in a permanent magnet whose pole faces were shimmed so that the field inhomogeneity across the sample was approximately 50 gauss, corresponding to a "band width"

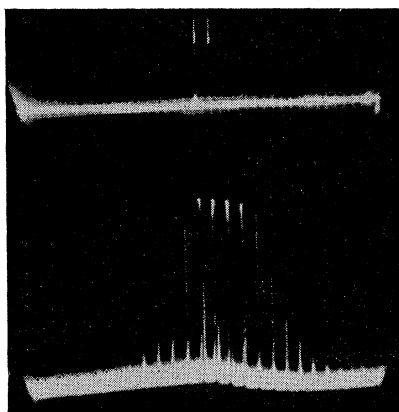
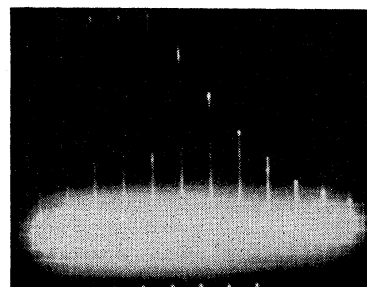
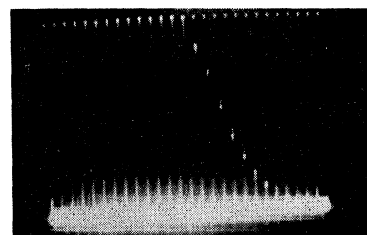


FIG. 7. Double pulses (above) and echoes preceding and following pulses (below). The receiver amplifier limits the amplitude of the stronger echoes. The double pulses were repeated in a time short compared to T_2 .

¹⁰ Bloch, Hansen, and Packard, Phys. Rev. 70, 474, (1946).



(a)



(b)

FIG. 8. Echoes at the end of a train of single pulses, indicated by the pips that follow an exponentially decaying curve. The repetition times for the pulses are 3 milliseconds (above) and 1 millisecond (below).

of 200 kc. The distribution of nuclei in this field was such that the polarization $g(\Delta\omega)$ was approximately constant over more than half of the total bandwidth. The bandwidths of the transmitter and receiver circuits were likewise about 200 kc. Although the direct coupling between transmitter and receiver in a crossed-coil probe tends to be frequency dependent, it was found possible to reduce the over-all coupling to the point where the rf pulses would not overload the receiver amplifiers.

In a magnetic field as inhomogeneous as the one used here, the effects of self-diffusion severely limit the time in which one can do echo and pulse-train experiments. Experiments involving only a few pulses can be done in ten milliseconds or less; for this a fairly viscous material, such as glycerine or SAE-30 motor oil, is useful. Experiments involving repeated pulses require longer times; for these the best sample material is a relatively nonviscous liquid in a fairly viscous emulsion. Most of the photographs shown here were taken with a sample of water mixed in lanolin, of the type used in cosmetic-cream preparations.¹¹ Even so, the lifetime for two-pulse echoes before disappearance under self-diffusion effects was only about 60 milliseconds.

¹¹ S. Fernbach and W. G. Proctor, J. Appl. Phys. 26, 170 (1955).

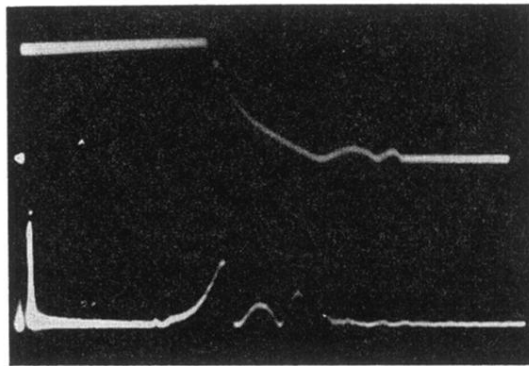


FIG. 4. Free decay (above) and echo (below) when $\gamma H_1 t_1 \approx 4\pi$.

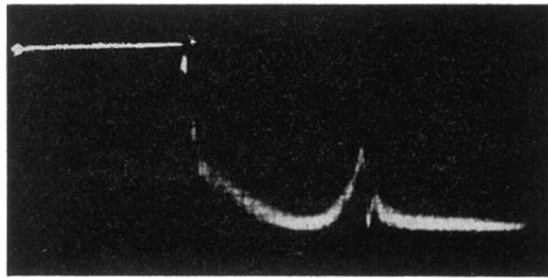


FIG. 5. Free decay and edge echo following single pulse. The pulses were repeated in a time short compared to T_2 .

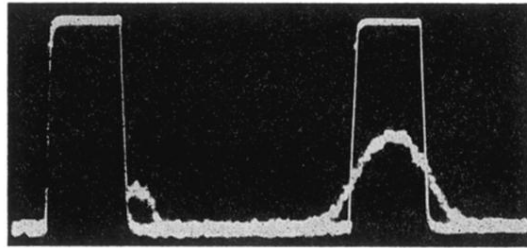


FIG. 6. Superpositions of first pulse, second pulse, and echo showing exact timing of echo maximum.

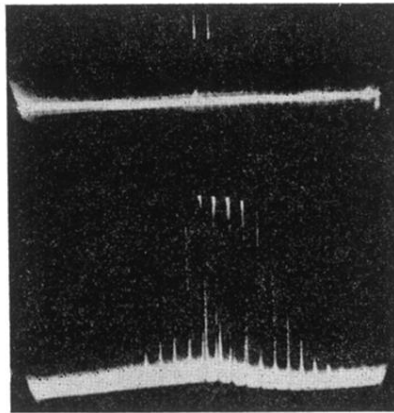
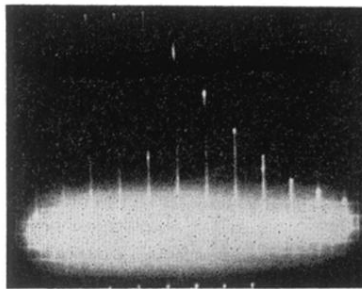
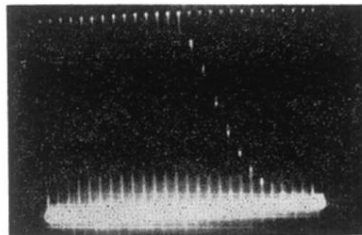


FIG. 7. Double pulses (above) and echoes preceding and following pulses (below). The receiver amplifier limits the amplitude of the stronger echoes. The double pulses were repeated in a time short compared to T_2 .



(a)



(b)

FIG. 8. Echoes at the end of a train of single pulses, indicated by the pips that follow an exponentially decaying curve. The repetition times for the pulses are 3 milliseconds (above) and 1 millisecond (below).